Journal for ImmunoTherapy of Cancer

Targeted inhibition of Aurora kinase A promotes immune checkpoint inhibition efficacy in human papillomavirus-driven cancers

Soma Ghosh,[1] Madison P O'Hara,[1,2] Pragya Sinha,[1,3] Tuhina Mazumdar,[1] Lacin Yapindi,[1] Jagannadha K Sastry ,[1,4] Faye M Johnson [1,4]

To cite: Ghosh S, O'Hara MP, Sinha P, *et al*. Targeted inhibition of Aurora kinase A promotes immune checkpoint inhibition efficacy in human papillomavirus-driven cancers. *Journal for ImmunoTherapy of Cancer* 2025;**13**:e009316. doi:10.1136/jitc-2024-009316

► Additional supplemental material is published online only. To view, please visit the journal online (https://doi.org/10.1136/jitc-2024-009316).

SG and MPO contributed equally.

Accepted 05 December 2024

[1]Department of Thoracic, Head and Neck Medical Oncology, The University of Texas MD Anderson Cancer Center, Houston, Texas, USA
[2]The University of Texas at Austin College of Pharmacy, Austin, Texas, USA
[3]Eikon Therapeutics Inc, Hayward, California, USA
[4]The University of Texas Graduate School of Biomedical Sciences, Houston, Texas, USA

Correspondence to
Dr Faye M Johnson;
fmjohns@mdanderson.org

ABSTRACT

Background Human papillomavirus (HPV)-driven cancers include head and neck squamous cell carcinoma and cervical cancer and represent approximately 5% of all cancer cases worldwide. Standard-of-care chemotherapy, radiotherapy, and immune checkpoint inhibitors (ICIs) are associated with adverse effects and limited responses in patients with HPV-driven cancers. The integration of targeted therapies with ICIs may improve outcomes. In a previous study, we demonstrated that Aurora kinase A (*AURKA*, Aurora A) inhibitors lead to apoptosis of human HPV-positive cancer cells in vitro and in vivo. Here, we explored the potential of Aurora A inhibition to enhance response to ICIs in immune-competent preclinical models of HPV-driven cancers.

Methods We assessed the induction of apoptosis, DNA damage, and immunogenic cell death (ICD) in response to treatment with the Aurora A inhibitor alisertib in vitro and antitumor efficacy of alisertib as a monotherapy and in combination with ICIs that inhibit programmed cell death protein-1 (PD-1) or cytotoxic T-lymphocyte associated protein 4 (CTLA-4) in murine HPV-positive immune-competent tumor models. In each treatment group, we determined the tumor growth kinetics and long-term survival and assessed the tumor immune microenvironment using polychromatic flow cytometry.

Results Aurora A inhibition induced apoptosis, DNA damage, and ICD in vitro in multiple human and murine HPV-positive cancer cell lines. Importantly, Aurora A inhibition induced selective apoptotic depletion of myeloid-derived suppressor cells (MDSCs). In vivo experiments demonstrated that the combination of alisertib with ICIs, specifically anti-CTLA4, resulted in improved survival outcomes by altering the tumor immune microenvironment. This combination enhanced CD8 T-cell infiltration and decreased the frequencies of MDSCs, whereas neither alisertib nor ICIs (anti-PD-1/anti-CTLA-4) alone showed such effects.

Conclusion Our study establishes the potential of Aurora A inhibition to sensitize HPV-positive tumors to ICIs, specifically anti-CTLA-4 treatment. This combination strategy resulted in enhanced antitumor efficacy, driven by systemic and intratumoral increases in CD8 T-cell responses and reduced immunosuppressive cell populations, specifically MDSCs. These findings offer insights into the synergistic effects of Aurora A inhibition and ICIs and argue for further investigation and optimization of this combination approach in HPV-driven cancers.

WHAT IS ALREADY KNOWN ON THIS TOPIC

⇒ Human papillomavirus (HPV)-driven cancers, accounting for 5% of global cancer cases, have limited responses to standard treatments (chemotherapy, radiotherapy, and immune checkpoint inhibitors), which has prompted exploration of targeted therapy combinations to enhance outcomes.

WHAT THIS STUDY ADDS

⇒ Inhibiting Aurora kinase A led to immunogenic cell death in HPV-driven cancers and sensitized them to anti-cytotoxic T-lymphocyte associated protein 4 (CTLA-4) treatment, leading to improved antitumor efficacy through increased systemic and intratumoral CD8 T-cell responses and reduced immunosuppressive myeloid-derived suppressor cell populations.

HOW THIS STUDY MIGHT AFFECT RESEARCH, PRACTICE OR POLICY

⇒ Our study shows that combining an Aurora kinase inhibitor with anti-CTLA-4 treatment could address immune evasion and potential metastasis through immune system suppression and be a promising treatment for HPV-positive cancers.

INTRODUCTION

Human papillomavirus (HPV) infections can cause head and neck squamous cell carcinoma (HNSCC) and genital cancers. The incidence of HPV-positive HNSCC is increasing in the USA and worldwide.[1] Locally advanced HPV-positive cancers are treated with a combination of radiotherapy and platinum chemotherapy. However, these treatments can induce adverse effects that can decrease quality of life, including irreversible deficits in swallowing, dry mouth, reliance on feeding tubes, and aspiration pneumonia.[2]

Systemic treatments for recurrent or metastatic HPV-positive HNSCC include platinum-based chemotherapy, immune checkpoint inhibitors (ICIs) targeting programmed cell death protein-1 (PD-1), and cetuximab, a monoclonal antibody that targets the epidermal growth factor; these systemic treatments can be given as single agents or in combination.[3] The approval of PD-1 inhibitors for frontline treatment of recurrent or metastatic cancer resulted in a paradigm shift in the treatment landscape for patients. That approval was based on the results of the KEYNOTE-048 trial, in which the median overall survival (OS) for the PD-1 inhibitor (pembrolizumab alone) was longer than that for the standard-of-care treatment (cetuximab and chemotherapy) in both the patients with a combined positive score of 20 or above (14.7 vs 11 months; p=0.004) and patients with a combined positive score of 1 or above (13.6 vs 10.4 months; p=0.001).[4] Similar results were observed in anal and cervical cancers.[5–7]

While ICIs offer clear benefits, only some patients with HNSCC respond to them.[4 8 9] Approximately 80% of recurrent or patients with metastatic HNSCC do not respond to ICI and the median OS is still less than a year[4 9] and, a significant number of patients with advanced disease either fail or progress on single-modality checkpoint inhibitor therapy. Therefore, newer, more effective therapeutic approaches are required.

One strategy to improve outcomes is to enhance the efficacy of ICIs. Although targeted therapy and chemotherapy increase survival and improve quality of life, nearly all patients with recurrent or metastatic solid tumors treated with ICIs eventually experience progression.[9] Conversely, some patients with recurrent or metastatic cancer treated with ICIs have complete and durable responses.[10–13] The genetic changes within tumors that initiate cancer growth present a chance to both suppress cancer-promoting signals and enhance immune response, thereby making tumors more responsive to ICIs. However, little information exists about the targeted agents that could synergize with ICIs in HPV-driven squamous cancers. One way to overcome resistance to immunotherapy may be to induce immunogenic cell death (ICD)—that is, to make the cancer cells "visible" to the immune system and attract T cells into the tumor immune microenvironment (TIME). ICD leads to the expression of calreticulin on the tumor's cell surface as an "eat-me" signal and to the release of damage-associated molecular patterns, proinflammatory cytokines, and tumor antigens into the TIME. Antigenic fragments are engulfed, processed, and presented by antigen-presenting cells such as dendritic cells to induce antigen-specific T-cell responses.[14] During pyroptosis, a form of ICD, the intrinsic apoptosis pathway leads to caspase-3 cleavage that induces gasdermin cleavage and the subsequent formation of a membrane pore that releases damage-associated molecular patterns.[15] Additionally, cancer -therapeutics may cause DNA damage and activate the c-GAS-STING pathway, leading to the production of type I interferons.

In a previous study, we tested the cytotoxic effects of 864 unique drugs in HPV-positive and HPV-negative human squamous cancer cell lines and identified Aurora kinase inhibitors as the only drug class that was more effective in HPV-positive cancer models than HPV-negative cancer models in vitro and in vivo.[16] Our and others' studies have shown that inhibiting Aurora kinase activity with reagents such as alisertib can lead to irreversible mitotic arrest, DNA damage, and apoptosis.[16 17] Moreover, the administration of alisertib has been documented to prompt senescence in melanoma cells, consequently augmenting the recruitment of tumor-infiltrating leukocytes (TILs).[18] However, limited knowledge exists regarding the specific impact of inhibiting Aurora kinase A (*AURKA*, Aurora A) on the TIME in HPV-driven cancers. Gaining a comprehensive understanding of the mechanism that drives the efficacy of Aurora A inhibition in HPV-positive cancers will pave the way for designing more effective therapeutic interventions using Aurora A inhibitors.

We hypothesized that the Aurora A inhibitor alisertib may augment the efficacy of ICIs in the treatment of HPV-driven cancers. In this study, leveraging our understanding of alisertib's specificity toward Aurora A inhibition and alisertib's demonstrated safety profile in human clinical trials,[19 20] we investigated the potential of Aurora A inhibition to induce ICD and promote the efficacy of ICI therapy in immune competent-mouse models of HPV-associated cancers.

Our experimental approach involved using well-established mouse models (mEER, C3.43, and TC-1), which serve as robust surrogates for HPV-driven HNSCC and genital cancers.[21–23] Building on previous work showing alisertib's ability to promote chromosome alignment and antitumor efficacy in preclinical models,[24] we sought to explore alisertib's potential synergy with ICIs targeting PD-1 or cytotoxic T-lymphocyte associated protein 4 (CTLA-4). In our study, we found compelling evidence that alisertib significantly enhances the antitumor efficacy of ICIs targeting PD-1 or CTLA-4 in the mEER model. This enhancement was associated with selective depletion of myeloid-derived suppressor cells (MDSCs). Our findings provide evidence to support that Aurora kinase-targeted therapy is a viable approach to augment the effectiveness of immune-based therapies for HPV-driven cancers.

MATERIALS AND METHODS

Cell lines

Human HNSCC and cervical squamous carcinoma cell lines (UMSCC47, SIHA, and CASKI) were obtained, maintained, and profiled as described previously.[25]

Mouse tonsil epithelial cells expressing HPV-16 *E6* and *E7* and *Hras1* oncogene (mEER) were a gift from Dr J Lee (Sanford Health, Sioux Falls, South Dakota, USA). These cells were preserved and maintained as described previously[26] and cultured to 80% confluency the day before implantation in mice. C3.43 cells, mouse embryonic

epithelial cells expressing the entire HPV-16 genome,[27] were provided by Dr M Kast (University of Southern California, Los Angeles, California, USA). These cells were grown and expanded in vitro in Iscove's Modified Dulbecco's Medium supplemented with 10% fetal bovine serum (Gemini, Sacramento, California, USA), 50 µM 2-mercaptoethanol, and 50 µg/mL gentamicin. Dr T C Wu and C Hung (Johns Hopkins School of Medicine, Baltimore, Maryland USA) provided the TC-1-luciferase (TC-1–Luc) tumor cell line. TC-1-Luc was derived from C57BL/6 mouse lung fibroblasts that were transfected to stably express *Hras1*, firefly luciferase, and HPV-16 *E6* and *E7*.[28] TC-1-Luc cells were maintained in Roswell Park Memorial Institute Medium (RPMI) 1640 medium supplemented with 50 units/mL penicillin-streptomycin, and 50 µg/mL gentamycin, and 10% heat-inactivated fetal bovine serum.[23]

All cell lines were genotyped using short tandem repeat analysis and were determined to be *Mycoplasma*-free using a MycoAlert Mycoplasma Detection Kit (Lonza, Morristown, New Jersey, USA).

REAGENTS

Alisertib was purchased from Selleck Chemicals and prepared as a 10 mmol/L stock solution in dimethyl sulfoxide (DMSO). Anti-PD-1 (RMP1–14 at 250 µg per dose) and anti-CTLA-4 antibodies (9H10 at 100 µg per dose) for in vivo administration were procured from Bio X Cell (West Lebanon, New Hampshire, USA). All the antibodies used for immunoblotting (western blot) and flow analyses are listed in online supplemental tables S1 and S2.

Immunoblotting

Immunoblotting was performed as described previously.[29] In brief, cells were lysed with ice-cold lysis buffer, and the lysates were centrifuged at 20,000×g for 10 min at 4°C. Protein concentrations were assessed using bicinchoninic acid assay (Thermo Scientific, Waltham, Massachusetts, USA).[30] Cell lysates containing equal amounts of protein were resolved using sodium dodecyl sulfate-polyacrylamide gel electrophoresis and transferred to nitrocellulose membranes. Protein presence and abundance on the nitrocellulose membranes were determined through Ponceau S staining (0.5% w/v Ponceau S dissolved in 1% v/v acetic acid). Following a 5 min incubation in the Ponceau S solution, the membranes were washed once with water, photographed, and subsequently destained Tris-buffered saline with 0.1% Tween 20 detergent. Subsequently, the membranes were incubated with the indicated primary antibodies (online supplemental table S1). Protein expression was detected using a horseradish peroxidase-conjugated secondary antibody (Bio-Rad, Hercules, California, USA) and enhanced chemiluminescence reagent (Thermo Scientific). For the quantification of protein expression, the band intensities were measured using ImageJ, RRID:SCR_003070 (National Institutes of Health, Bethesda, Maryland, USA),[31] and normalized first to actin and then to its respective positive control.

Analysis of apoptosis, cell-surface calreticulin expression, and cell viability

To measure apoptosis, we performed annexin V/propidium iodide staining with an fluorescein isothiocyanate (FITC) Annexin V Apoptosis Detection Kit (eBioscience, San Diego, California, USA) as described previously.[16] Briefly, cells were treated with 300 nM alisertib for 48 hours on the basis of findings from our earlier studies.[16] After treatment, the cells were collected, washed twice with ice-cold phosphate-buffered saline (PBS), and resuspended in 1 mL of annexin binding buffer (10 mM HEPES/NaOH, pH 7.4; 140 mM NaCl; 2.5 mM $CaCl_2$). The cell suspension (approximately 1×10^5 cells) was transferred to a 5 mL fluorescence-activated cell sorting (FACS) tube and mixed with 5 µL of annexin V-FITC. The cells were gently vortexed and incubated for 20 min at 25°C in the dark. After the incubation, samples were washed with annexin binding buffer for 5 min. Once samples were washed, 200 µL of binding buffer with propidium iodide was added to each sample, which was then analyzed using a Beckman Coulter Gallios flow cytometer.

Cell viability was assessed using the CellTiter-Glo Luminescent Cell Viability Assay (G7570, Promega) according to the manufacturer's instructions. Cells were grown in 96-well plates and treated with 300 nM alisertib for 48 hours. Following treatment, 100 µL of CellTiter-Glo reagent was added to each well. Luminescence was measured using a BioTek Microplate Reader (BioTek Instruments, Winooski, Vermont, USA).

Cell surface calreticulin was analyzed in human and murine samples following alisertib treatment. Briefly, the cells were treated with 300 nM alisertib for 48 hours at 37°C; washed twice with cold PBS; and then incubated with 1 µL of ZombieAqua (Thermo Scientific), an amine-reactive fluorescent viability dye, for 20 min in the dark at room temperature. Subsequently, the cells were washed and incubated with 100 µL of diluted (1:100) anti-calreticulin phycoerythrin-conjugated antibody (Cell Signaling Technology; Danvers, Massachusetts, USA) at 4°C for 30 min. Cells were analyzed on a Beckman Coulter Gallios flow cytometer.

In vivo mouse studies

Sample size calculations were based on preliminary data with a primary endpoint of tumor weight at the end of the study and an assumption that alisertib would have an effect similar to that of the single agent anti-PD-1 antibody (Ab) and that the drug combination would have an effect size of 0.83. A sample size of seven mice per group achieves 88% power to detect tumor volume differences among the four treatment groups using one-way analysis of variance (ANOVA) with a 0.05 significance level. Syngeneic male C57BL/6 mice, 6 weeks old, were implanted

with 1×10^6 mEER cells in 200 µL PBS subcutaneously on the right flank as reported previously.[21 22] After tumors reached an average size of 50–70 mm^3, the mice were randomized into different treatment groups, with seven mice per group. In the combination group (alisertib with anti-PD-1 or alisertib with anti-CTLA-4), we included eight mice per group. Alisertib (from Takeda Pharmaceuticals; 10 mg/kg in 10% β-cyclodextrin) was administered orally through gavage. Mice were monitored twice weekly for body weight changes and tumor growth. Mice were euthanized when they lost 20% or more of their initial body weight or when the tumor size exceeded 200 mm^2. For the experiments involving analysis of TILs, 1×10^6 mEER tumor cells in PBS were mixed in a 2:1 ratio with Matrigel (BD Biosciences, San Jose, California, USA) for implantation. For the immune correlates analysis for the alisertib and anti-PD-1 experiments we included five mice per group.

Immune cell isolation

On indicated days after the tumor cell implantation, mice were euthanized, and tumors and spleens were collected to assess cell-mediated antitumor immune responses as previously described.[22 23] Briefly, tumors were digested in a complete RPMI medium containing collagenase H (Sigma-Aldrich, St. Louis, Missouri, USA) and DNase (Roche, Indianapolis, Indiana, USA) and incubated at 37°C for 45 min before being passed through 70 µm cell strainers. The TILs were isolated using 67%:44% Percoll (Cytiva, Marlborough, Massachusetts, USA) gradient centrifugation. Single-cell suspensions from spleens were prepared by mechanical disruption and passing the cells through cell strainers; these analyses were followed by red blood cell lysis.

For characterization of circulating lymphocytes, blood was collected from mice via the retroorbital technique.[32] Whole blood was incubated at 37°C and 5% CO_2 for 5 min with Tris-buffered ammonium chloride buffer (130 mM Tris and 150 mM NH_4Cl in a 1:9 ratio) to lyse red blood cells and then was washed with PBS. In addition to blood, spleens were also harvested, minced, and the cells were washed with PBS/2% fetal bovine serum (FBS). Red blood cells were lysed with NH_4Cl lysis buffer, followed by washing with PBS/2% FBS and filtration through strainers to isolate lymphocytes for further analysis.

Flow cytometry

Following isolation, cells were incubated at 37°C and 5% CO_2 for 4–6 hours with brefeldin A GolgiPlug (Thermo Fisher). Cells were blocked using mouse Fc-block (anti-CD16/32) (Thermo Fisher), stained for surface markers using a cocktail of fluorescently labeled antibodies (online supplemental table S2), fixed, and permeabilized and then stained for intracellular/functional markers.[21–23 33] FACS data acquisition was done on a five-laser Fortessa X-20 flow cytometer (BD Biosciences), and data were analyzed using FlowJo V.10 (Ashland, Oregon, USA). Forward and side scatter parameters were used to set singlets and leukocyte gates. Fixable viability stain 510 was included in the surface antibody cocktail and used to gate out dead cells so that only viable cells were analyzed. The HPV antigen-specific CD8 T cells were detected using the HPV-16 E7 CD8 T-cell epitope tetramer reagent from Emory University NIH MHC tetramer core facility (Atlanta, Georgia, USA) that was part of the multiparametric flow cytometry panel. For the detection of MDSC, a gating strategy involving CD3-CD11b+Gr-1+ was used.

Statistical analysis

All graphing and statistical analyses were performed using GraphPad Prism V.8 (San Diego, California, USA). One-way ANOVA followed by Tukey post hoc test was used for comparing multiple groups, and an unpaired, two-tailed Student's t-test was used for comparing two groups. Statistical significance between survival curves was calculated using a log-rank test (Mantel-Cox). A p value of <0.05 was considered significant. Graphs show the mean±SD values for each group unless otherwise indicated. Experiments were repeated to confirm the reproducibility of the results.

RESULTS

Aurora kinase A inhibition induced apoptosis, DNA damage, and ICD and reduces cell viability in HPV-positive murine and human cancer cell lines in vitro

We tested the effect of the Aurora A inhibitor alisertib in three different human HPV-positive cancer cell lines (UMSCC47, SIHA, and CASKI) and three different murine HPV-positive tumor cell lines (mEER, C3.43, and TC-1). All the cell lines were treated with 300 nM alisertib for 48 hours on the basis of conditions optimized in previous studies.[16]

As expected, alisertib treatment markedly reduced phospho-Aurora A protein expression levels (online supplemental figure 1A). We also observed a modest increase in total Aurora A protein levels in cells treated with alisertib, which may have been due to the increased accumulation of cells in the G2-M phase of the cell cycle. Alisertib-treated cells had increased caspase-3 activation and poly(ADP-ribose) polymerase (PARP) cleavage (figure 1A) and enhanced annexin V-positive cell staining (figure 1B), showing that alisertib induced apoptosis. To assess the effects of alisertib on cell survival, we performed a cell viability assay. As shown in figure 1C, both murine and human HPV-positive cell lines exposed to alisertib exhibited a significant reduction in cell viability after 48 hours of treatment. This decrease in viable cells aligns with the observed apoptotic markers and provides additional evidence for the cytotoxic efficacy of alisertib in these HPV-positive cancer cell lines.

In all cell lines, Aurora A inhibition activated the DNA damage pathway via a significant increase in the levels of phosphorylated H2A histone family member X (γ-H2AX) and phosphorylated TIF1β, which is known for its role in DNA damage (figure 1D,E). We also observed

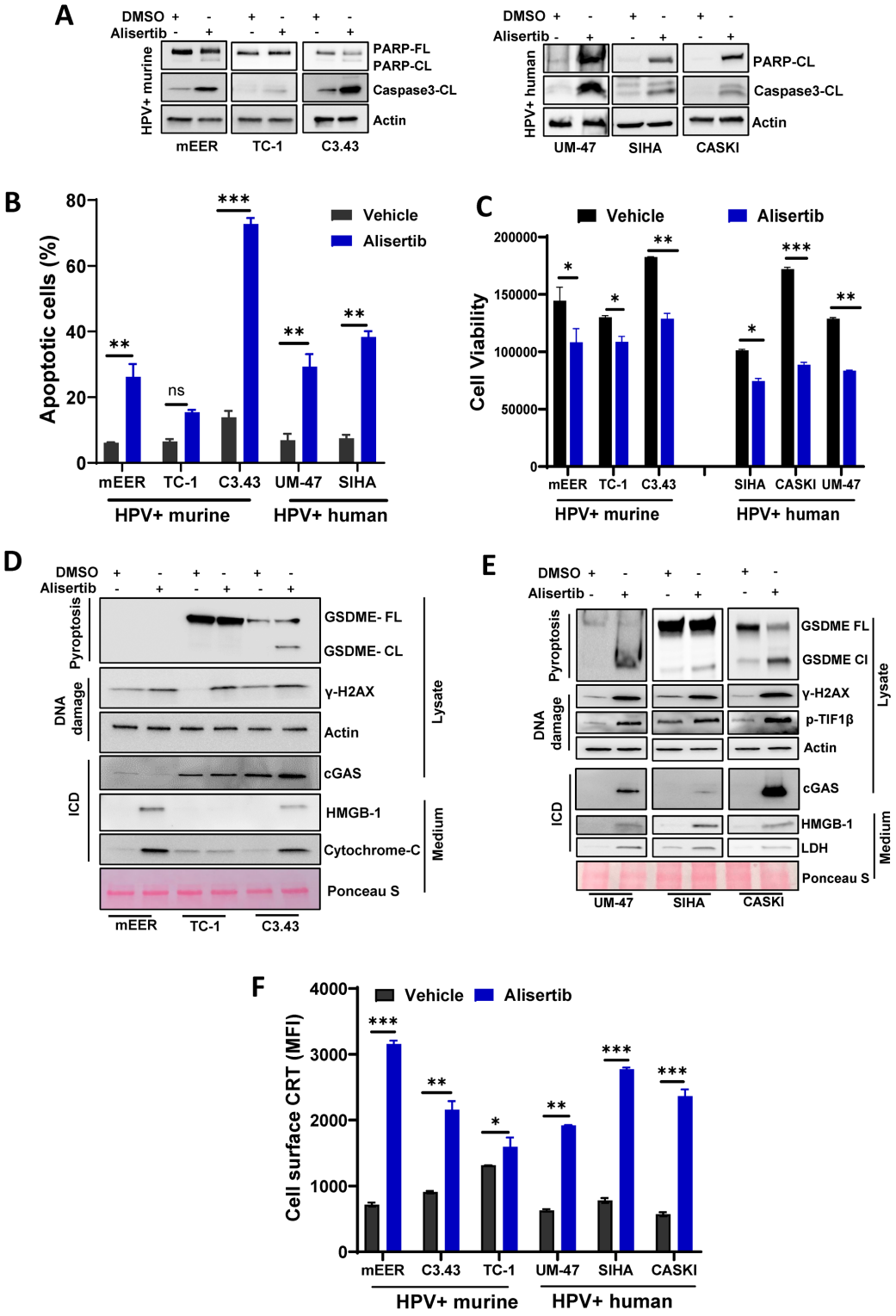

Figure 1 Aurora kinase A inhibition induces cytotoxicity, apoptosis, DNA damage, and immunogenic cell death in human papillomavirus (HPV)-positive murine and human cancer cell lines in vitro. (A–C) Murine and human cancer cells were treated with 300 nmol/L alisertib for 48 hours before being subjected to lysis and immunoblotting with the indicated antibodies (A), annexin-FITC staining to measure apoptosis (B), or a CellTiter-Glo assay to measure cell viability (C). (D–E) Murine (D) and human (E) cells were treated with 300 nmol/L alisertib for 48 hours before immunoblotting with antibodies that indicate the presence of pyroptosis, DNA damage, and immunogenic cell death (ICD). To determine the amount of released HMGB-1 (D, E), cytochrome C (D), and lactate dehydrogenase (LDH) (E), equal volumes of conditioned medium were subjected to immunoblotting analysis; Ponceau S staining was used as a loading control. (F) Calreticulin (CRT) expression on the cell surface was analyzed by flow cytometry on murine and human cell lines treated with 300 nmol/L alisertib for 48 hours. The significance of differences was determined using an unpaired, two-tailed Student's t-test. *p≤0.05, **p≤0.001, ***p≤0.0001. CL, cleaved; DMSO, dimethyl sulfoxide; FL, full; GDSME, gasdermin E; MFI, mean fluorescence intensity; UM-47, UMSCC47.

marked activation of the cGAS/STING pathway in both human and murine HPV-positive tumor cells treated with alisertib, which can be stimulated by DNA damage.

In addition to apoptosis, activated caspase-3 mediates the cleavage of gasdermin E which leads to pyroptosis,[34] a form of ICD that can reverse immunotherapy resistance. Alisertib treatment led to gasdermin E cleavage in C3.43 murine HPV-positive cells (figure 1D) as well as in all the human HPV-positive tumor cells tested (figure 1E). However, mEER cells did not express gasdermin E. Gasdermin D and gasdermin F (PVJK) were not detected in any of the cell lines studied (data not shown). Additionally, Aurora A inhibition led to the release of damage-associated molecular patterns (cytochrome C, HMGB-1, and lactate dehydrogenase), which are hallmarks of ICD, into the cell supernatant (figure 1D,E).

An initial hallmark of ICD involves the externalization of calreticulin, resulting in the relocation of endoplasmic reticulum-resident calreticulin to the plasma membrane.[35] The presence of surface calreticulin serves as an "eat me" signal, which is crucial for triggering immune cells and priming the innate immune response.[36] Using flow cytometry, we detected a significant accumulation of calreticulin on the cell surface after 48 hours of treatment with alisertib in all the human and murine tumor cell lines tested (figure 1F, online supplemental figure S2). These results establish that alisertib induced ICD in HPV-positive tumor cells via distinct cell death mechanisms and support in vivo antitumor efficacy assessment.

Aurora A inhibition induced a transient decrease in tumor growth and functional MDSCs in HPV-driven tumors in vivo

To test the effects of Aurora kinase inhibition in vivo, we administered alisertib (10 mg/kg), using a clinically relevant dose and regimen[24 37] daily via oral gavage to mice with mEER tumors for 6 days then monitored mice for tumor growth and survival over the next 50 days (figure 2A). Although mice treated with alisertib had significantly reduced tumor weight at day 25 compared with the weight of mice in the control group (figure 2B), the tumors progressed in all the mice, with no significant difference in survival between the groups (figure 2C).

Analyses of blood collected at days 7, 13, 18, and 25 showed significantly higher levels of total and HPV E7 antigen-specific CD8 T cells (figure 2D,E,G,H) at day 18 (figure 2E,H insets) in mice treated with alisertib that was preceded by a significant drop in the levels of MDSCs at day 13 (figure 2J,K insets) in mice treated with alisertib relative to the levels in mice in the control group. However, these differences were not sustained for any cell types by day 25. Similarly, although analyses of TILs from mice euthanized at days 13 and 25 showed no differences in the levels of total and HPV E7 antigen-specific CD8 T cells (figure 2F,I), a significant decrease in the frequencies of an arginase-positive functional subset of MDSCs were observed at day 13 (figure 2L, inset), although this difference was not sustained by day 25 (figure 2L).

Thus, alisertib treatment induced a transient decrease in tumor growth and changes in TILs, but these changes were not sustained over time, and no survival benefit was observed. The observation of a reduction in MDSCs but not total CD8 T cells and HPV E7 antigen-specific CD8 T cells in alisertib-treated mice was recapitulated in two other preclinical models (TC-1 and C3.43) and did not translate into a long-term survival benefit (online supplemental figure 3).

Aurora A inhibition led to selective induction of apoptosis in MDSCs but not CD8 T cells

To understand the mechanism driving the observed differential effects of alisertib treatment on MDSCs versus CD8 T cells, we conducted ex vivo experiments on spleen cells from mEER tumor-bearing mice. Alisertib treatment induced apoptosis in MDSCs but not CD8 T cells, as evidenced by significantly increased frequencies of annexin V^+ MDSCs but not CD8 T cells (figure 3A,B).

To further understand the mechanism driving alisertib's differential effects, we investigated the release of cytochrome C, which is a known key mediator of apoptosis.[38] Alisertib-treated MDSCs, but not CD8 T cells, exhibited higher secretion of cytochrome C than the vehicle control-treated cells did (figure 3C), indicating potential involvement of the apoptotic pathway in MDSC depletion.

Combination of Aurora A inhibition and PD-1 blockade extended the survival of mice bearing HPV-driven tumors

We previously reported that mice with mEER flank tumors were resistant to ICIs targeting PD-1.[21] Because we observed that Aurora A inhibition induced ICD in tumor cells in vitro (figure 1E), we tested whether Aurora A inhibition can effectively sensitize mice with mEER flank tumors to anti-PD-1 treatment in vivo. To test this hypothesis, mice bearing mEER flank tumors were treated with two cycles of anti-PD-1 monotherapy, alisertib monotherapy, a combination of anti-PD-1 treatment and alisertib, or a vehicle control and were monitored for tumor growth and survival over 60 days (figure 4A). On day 23, we observed a significant decrease in tumor size in mice treated with the combination (figure 4B), but eventually mice in all the groups exhibited sustained tumor growth (figure 4C). However, mice treated with the combination of alisertib and anti-PD-1 survived longer than those in the control and monotherapy groups (figure 4D). The median survival times were as follows: vehicle: 37.5 days, alisertib: 39 days, anti-PD-1: 42 days, and combination: 51 days. These results suggest that the combination therapy significantly improved survival compared with the vehicle and monotherapy groups, highlighting its potential for enhancing antitumor immunity. The frequencies of total and cytotoxic HPV E7 antigen-specific CD8 T cells (figure 4E,F) and regulatory T cells (Tregs) (figure 4G) were not significantly different among the groups. However, analyses of TILs showed significantly reduced levels of MDSCs in mice treated with

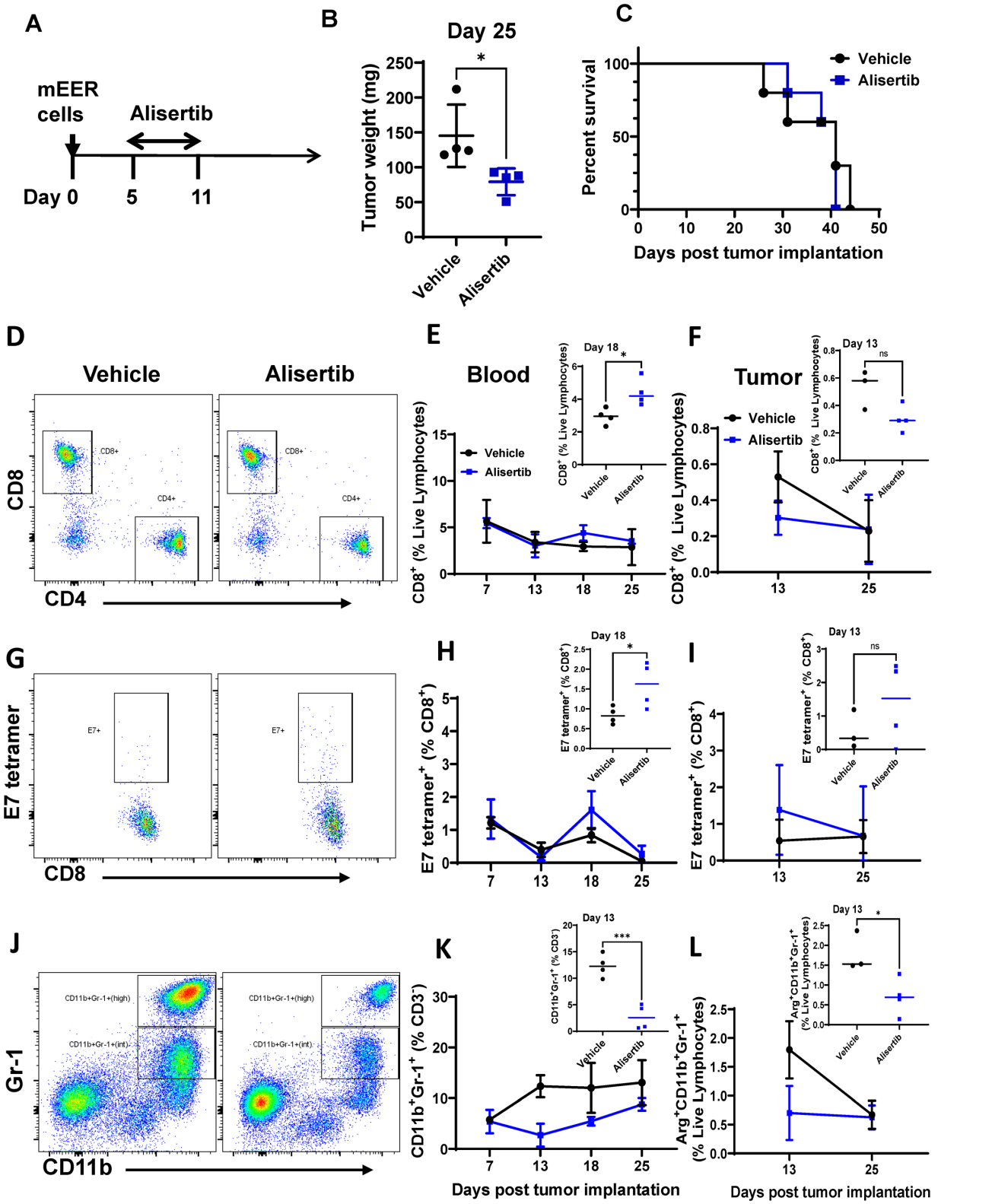

Figure 2 Aurora kinase A inhibition has differential effects on T cells and MDSCs in vivo in HPV-positive tumor-bearing mice. (A–C) Groups of C57BL/6 mice were implanted with mEER cells (1×10^6) subcutaneously on the flank and treated with alisertib (10 mg/kg) daily for 6 days starting at day 5 after tumor cell implantation (A) and monitored for tumor growth (weight) (B) and survival (C). (D–L) Changes in total CD8 T cells (D–F), HPV E7 antigen-specific CD8 T cells (G–I), and MDSCs ($CD11b^+$ $Gr\text{-}1^+$) (J–L) were monitored by flow cytometry at the indicated time points in the blood (day 18 for E7 and CD8 and day 13 for MDSCs) (E, H, K) and tumor (day 13 for MDSCs and day 25 for $E7^+$ and CD8 cells) (F, I, L). Representative flow profiles for CD8 T cells (D), HPV E7 antigen-specific CD8 T cells (G), and MDSCs (J) in the blood from vehicle-treated and alisertib-treated mice are shown. The significance of differences was determined using an unpaired, two-tailed Student's t-test. ns, $p\leq0.05$*, ***$p<0.009$. HPV, human papillomavirus; MDSCs, myeloid-derived suppressor cells.

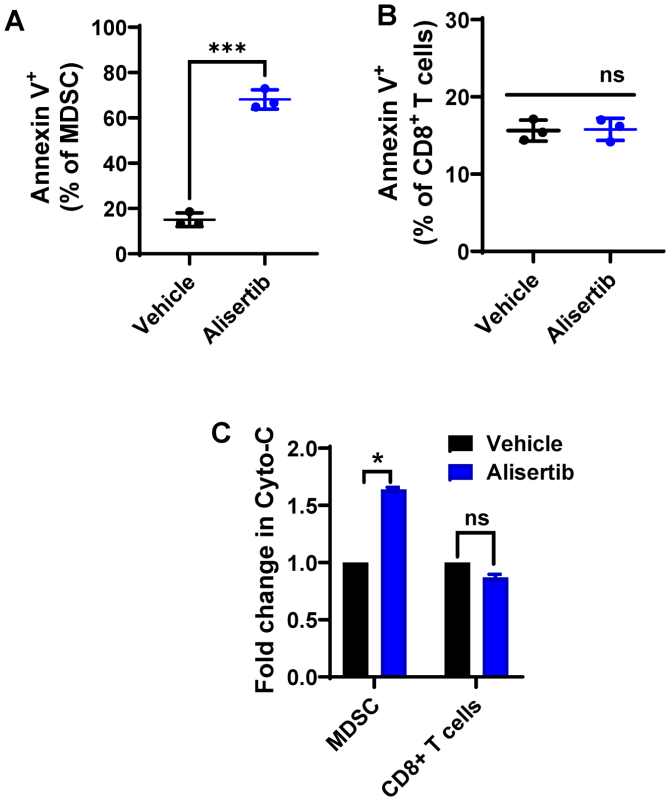

Figure 3 Aurora kinase A inhibition ex vivo induces apoptosis in HPV-positive tumor-induced MDSCs but not CD8 T cells. (A–B) Splenocytes isolated from mEER tumor-bearing mice were treated ex vivo with vehicle or alisertib (300 nM) for 6 hours, and apoptotic cells (annexin V$^+$) within the MDSC (A) and CD8 T cell (B) fractions were identified by flow cytometry. (C) MDSCs and CD8 T cells (C) from the mEER tumors were purified and treated ex vivo with vehicle or with alisertib (300 nmol/L) for 6 hours. Protein extracts were analyzed for apoptosis and survival pathway proteins using an antibody array. The significance of differences was determined using an unpaired, two-tailed Student's t-test. ns (not significant), *p≤0.01, **p≤0.004, ***p≤0.0001. Cyto-C, cytochrome C; HPV, human papillomavirus; MDSCs, myeloid-derived suppressor cells.

alisertib monotherapy or the combination of alisertib and anti-PD-1 (figure 4H).

Combination of Aurora A inhibition with CTLA-4 blockade significantly extended the survival of mice bearing HPV-driven tumors

In mEER tumors of both treated and untreated mice, we observed that the T-cell inhibitory coreceptor CTLA-4 was expressed at significantly higher levels than PD-1 on CD4 and CD8 T cells, Tregs, and natural killer cells. These elevated levels were consistent regardless of alisertib treatment (figure 5). This persistent overexpression of CTLA-4 relative to PD-1 suggests that CTLA-4 may be a better target for immunotherapy and we hypothesized that alisertib would synergize with anti-CTLA-4 treatment. To test this hypothesis, mice with mEER flank tumors were treated with four cycles of anti-CTLA-4 monotherapy, alisertib monotherapy, a combination of anti-CTLA-4 antibodies and alisertib, or a vehicle control (figure 6A), and were monitored for tumor growth and survival over 60 days. We observed a significant reduction in tumor volume at day 36 in mice that received the combination compared with all other groups (figure 6B), which translated into the combination group having significantly slower tumor growth and long-term survival relative to either treatment alone (figure 6C,D). The median survival times were as follows: vehicle: 36 days, anti-CTLA-4: 40 days, alisertib: 42 days, and combination: not reached. In the combination group, 75% (6/8) of the mice exhibited tumor-free survival for a period of 60 days. Subsequently, we investigated the TIME for the observed protective efficacy of the combination treatment on day 23 because this time point was when we had observed decreased tumor size in the combination group in our in vivo experiments (figure 7A,B). For rigor, we repeated this experiment with similar results. We observed a significant delay in tumor growth in the combination group by day 23, as shown in the tumor growth curve (online supplemental figure 4A). Detailed analyses of T-cell responses revealed enhanced polyfunctionality, with increased interferon-γ and granzyme production in TILs. Additionally, a higher percentage of CD8+T cells producing these cytokines was found in the spleens of combination-treated mice, emphasizing both local and systemic immune responses contributing to tumor shrinkage. We also noted significant changes in immune marker profiles, with reduced expression of the T-cell exhaustion marker LAG3 in the tumor, suggesting improved T-cell activation. Furthermore, an increase in CXCR3+CD4+ and CD8+ T cells in the TIME was observed, indicating enhanced recruitment of effector T cells. Observed treatment-mediated changes in the different lymphocyte subsets are comprehensively represented in the heatmap (figure 7C).

Additionally, we observed a significant reduction in the granulocytic subset of MDSCs (Gr-1+Ly6G+) in the tumors from the combination treatment group, with a more pronounced decrease in the Gr-1low Ly6G+subset, which is known to represent a highly suppressive MDSC population.[39] This shift in the myeloid compartment suggests changes in immune cell dynamics in both the tumor and spleen. These results are depicted in the scatter plot (figure 7D), with individual graphs for all immune subsets shown in online supplemental figure S4B–E.

Additionally, immunoblotting of tumor tissues from four mice per treatment group revealed significantly higher expression of cleaved caspase-3 and cleaved PARP in the alisertib-treated groups, supporting the induction of cancer cell apoptosis (figure 7E). Together, these findings suggest that the combination of alisertib and anti-CTLA-4 induces substantial changes in the immune landscape in addition to cancer cell death, contributing to enhanced antitumor efficacy and improved long-term survival.

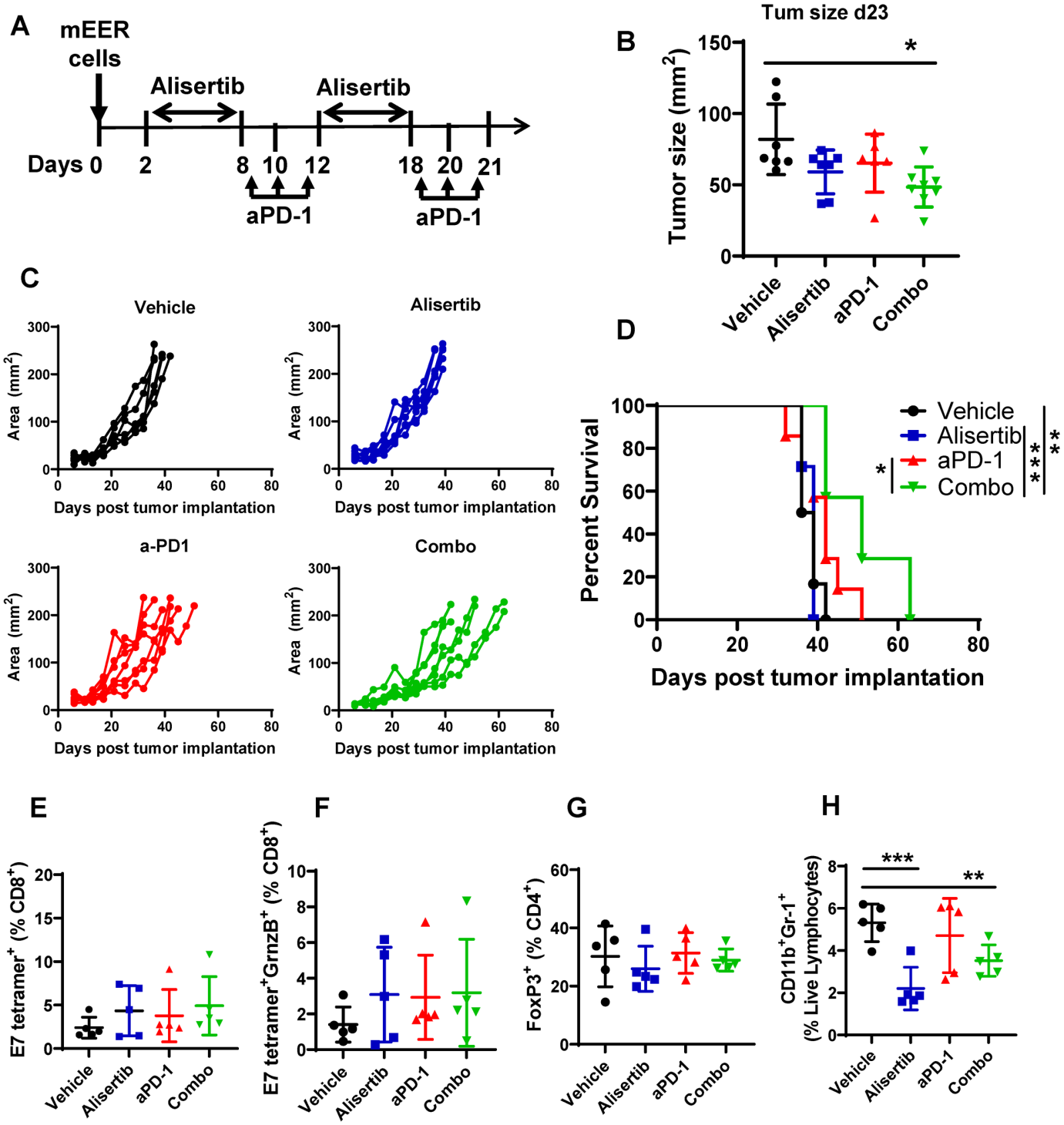

Figure 4 Aurora kinase A inhibition in combination with PD-1 blockade extends the survival of HPV-positive tumor-bearing mice. (A–D) Groups of C57BL/6 mice were implanted with mEER cells (1×10^6) subcutaneously on the flank and were treated sequentially with 10 mg/kg of alisertib and anti-PD-1 antibody (aPD-1) at 250 µg per dose individually or in combination (combo) as shown (A) and monitored for tumor growth (area) (B, C) and survival (D). Significant differences between the survival curves were determined using the log-rank Mantel-Cox test *p<0.05, **p<0.005, ***p<0.0005. (E–H) Tumor-infiltrating leukocytes were separated from tumors on day 23 after the tumor initiation when all the treatments were completed. Frequencies of total CD8 T cells (E), HPV E7 antigen-specific granzyme B-expressing ($GrnzB^+$) CD8 T cells (F), regulatory T cells ($FoxP3^+$) (G), and myeloid-derived suppressor cell (H) were measured using one-way analysis of variance. **p<0.005, ***p<0.0005. HPV, human papillomavirus; PD-1, programmed cell death protein-1.

DISCUSSION

To our knowledge, our research is the first to demonstrate that in HPV-positive tumors, Aurora A inhibition led to ICD. Furthermore, data from our study highlight that, in HPV-positive cancers, Aurora A inhibition enhanced the efficacy of ICIs targeting PD-1 or CTLA-4. Interestingly,

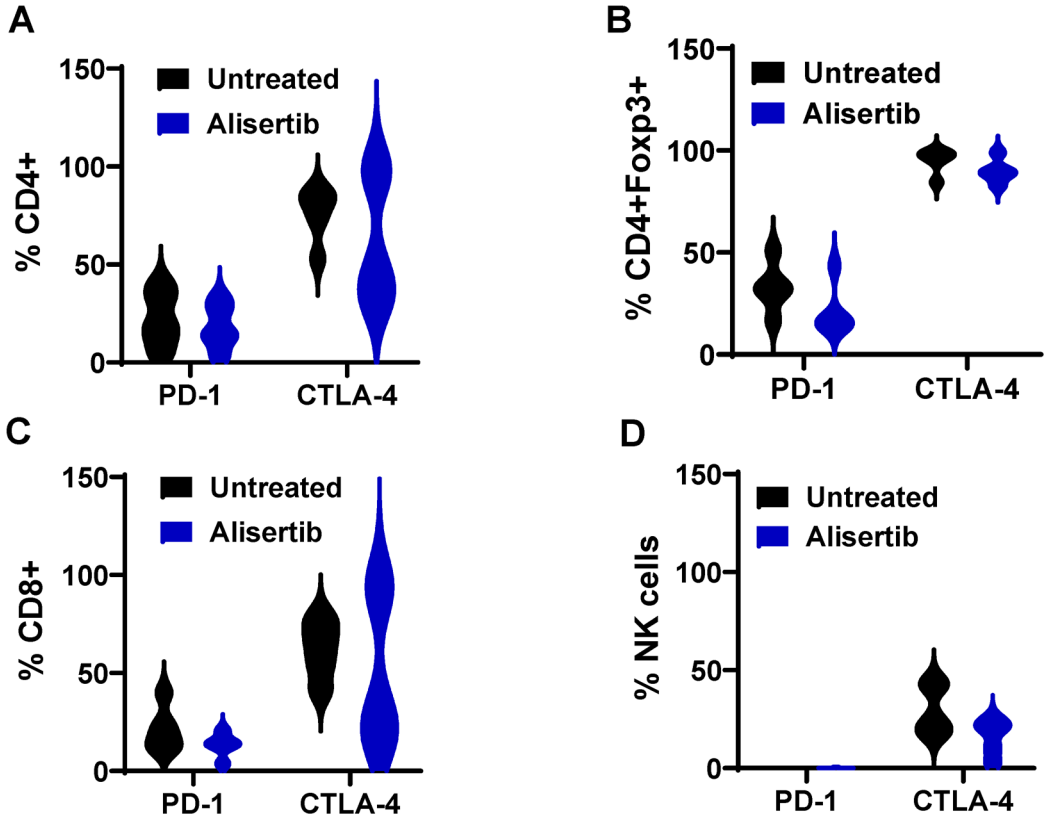

Figure 5 Aurora kinase A inhibition leads to persistently higher frequencies of CTLA-4-positive lymphocyte subsets than PD-1-positive lymphocyte subsets in mice with human papillomavirus-positive tumors. Single-cell suspensions of mEER tumor cells from vehicle-treated and alisertib-treated mice were analyzed by flow cytometry for the expression of PD-1 and CTLA-4 in $CD4^+$ (A), regulatory T (B), CD8 (C), and natural killer (NK) (D) cells. CTLA-4, cytotoxic T-lymphocyte associated protein 4; PD-1, programmed cell death protein-1.

the combination of alisertib and anti-CTLA-4 exhibited better antitumor efficacy than the combination of alisertib and anti-PD-1 treatment: The combination of alisertib and anti-CTLA-4 treatment resulting in tumor-free long-time survival of 75% of treated mice (figure 6C,D), while the combination of alisertib and anti-PD-1 treatment significantly extended OS (figure 4C,D).

Key mechanisms observed for the enhanced immune response in our study included a notable increase in the polyfunctionality of CD8+ and CD4+ T cells, accompanied by a reduction in MDSCs. In parallel with immune modulation, alisertib also significantly reduced cancer cell viability, which likely contributed to the enhanced antitumor efficacy observed. These responses were most pronounced in mice treated with the combination of alisertib and anti-CTLA-4 compared with those treated with control and monotherapies (figure 7). Interestingly, despite the significant changes in T cell and myeloid cell populations, we did not observe any significant alteration in the frequency of Tregs, both in the circulation and at the tumor site. While Tregs did not show significant changes in frequency, the primary mechanisms underlying the enhanced antitumor response appear to be the increased polyfunctionality of CD8+ and CD4+ T cells and the reduction of MDSCs. Notably, Tregs, despite expressing CTLA-4 (figure 5), may still contribute to immune suppression in other ways, such as through cytokine secretion or interactions with other immune cells, even though their frequencies remained unchanged.

Immunotherapy targeting CTLA-4 can include strategies that either block receptor activity or induce depletion of specific immune cell populations. The antibody used in our study, 9H10, is expected to have both blocking and depletion activities. However, based on our data showing no significant changes in Treg frequencies, it appears that in this HPV tumor mouse model, treatment with 9H10 primarily resulted in the blockade of CTLA-4 expression without leading to Treg depletion. This observation suggests that, at least in this model, CTLA-4 blockade was the dominant effect. While IgG2a antibodies like 9H10 are known to induce Treg depletion via antibody-dependent cellular cytotoxicity in other cancer models,[40–42] the effect in our study was more likely due to CTLA-4 blockade, which may play a more prominent role in this specific tumor model. Additionally, the effectiveness of CTLA-4 monoclonal antibodies has been shown to rely on their ability to directly activate CD8+T lymphocytes, contributing to the observed antitumor effects.[43] In our study, we observed a significant CD8+T cell response in the combination group, which may be due to the direct activation of CD8+TILs by anti-CTLA-4. Despite no significant changes in Treg frequency, the enhanced CD8+T cell activity likely

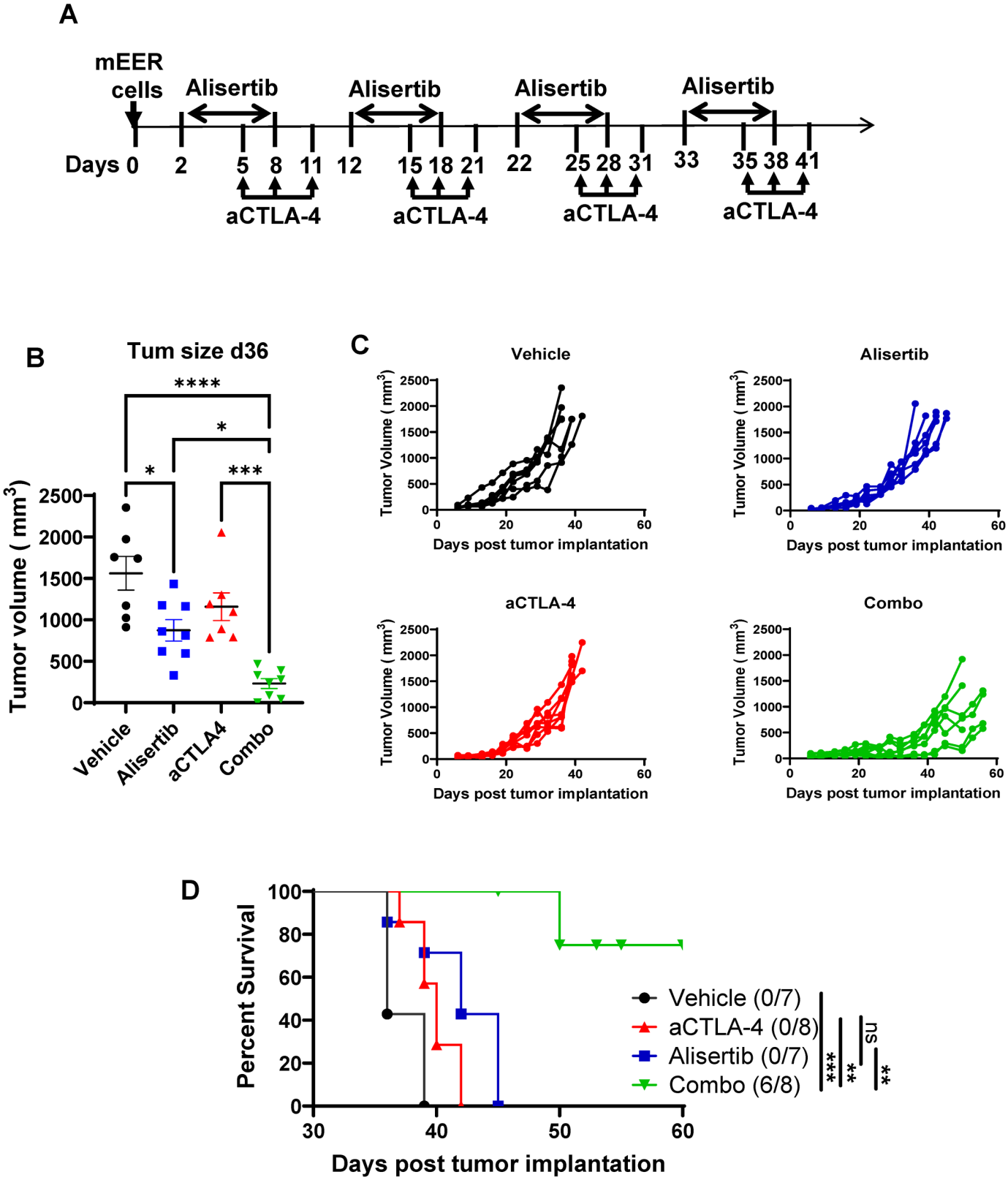

Figure 6 Aurora kinase A inhibition in combination with anti-CTLA-4 treatment extends the survival of human papillomavirus-positive tumor-bearing mice. Groups of C57BL/6 mice were implanted with mEER cells (1×10^6) subcutaneously on the flank and were treated sequentially with 10 mg/kg each of alisertib and anti-CTLA-4 antibody (aCTLA-4) individually or in combination (combo) (A) and monitored for tumor growth (B, C) and survival (D). Significant differences between the survival curves were determined using the log-rank (Mantel-Cox) test. ns, $p\geq0.05$, *$p<0.05$, **$p<0.005$, ***$p<0.0006$, ****$p<0.0001$. CTLA-4, cytotoxic T-lymphocyte associated protein 4.

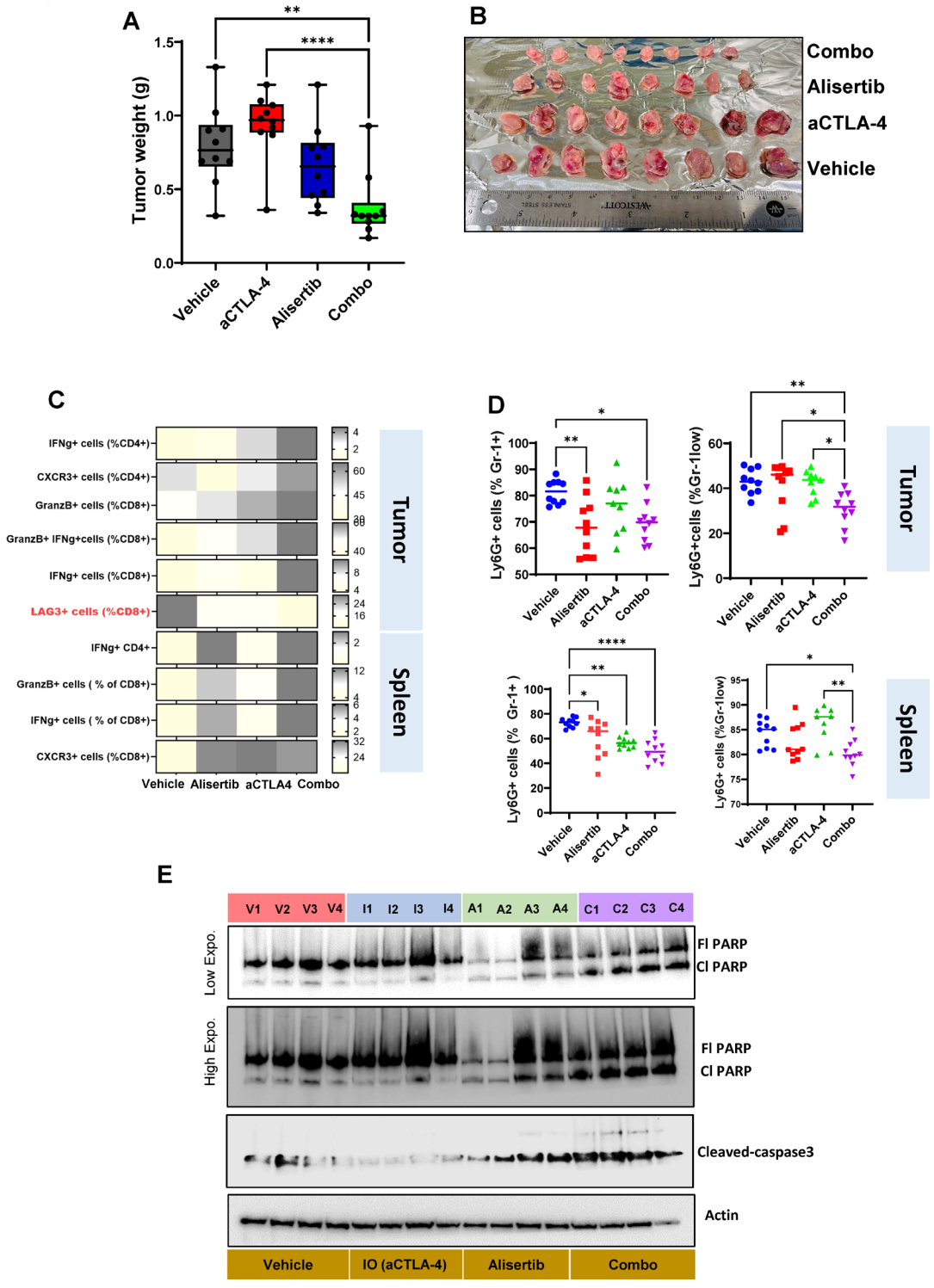

Figure 7 Aurora kinase A inhibition in combination with CTLA-4 blockade promotes antitumor immunity and cancer cell apoptosis. (A–B) Groups of C57BL/6 mice with mEER tumors were treated sequentially with alisertib (10 mg/kg) and anti-CTLA-4 antibody (aCTLA-4; 100 µg per dose) individually or in combination (combo). All mice were euthanized after two treatment cycles on day 23, and tumors were weighed (A, B). (C) Tumor-infiltrating lymphocytes and circulating lymphocytes from the tumor and spleen were isolated and analyzed by polychromatic flow cytometry to assess the frequencies of different immune cell populations. Changes in their expression are represented as a heatmap. The negative immune regulator LAG3 is highlighted in red. (D) Frequencies of circulating myeloid-derived suppressor cell levels for the tumor and spleen. The significance of differences in immune cell subsets among the treatment groups were assessed using one-way analysis of variance. *p<0.05, **p<0.005, ***p<0.0001, ****p<0.00005. (E) Immunoblotting was performed on tumor tissues from four mice per treatment group at day 23. The expression of cleaved caspase-3 (cl caspase-3), full-length PARP (Fl PARP), and cleaved PARP (cl PARP) were analyzed to assess apoptosis. The treatment groups are as follows: V – vehicle, I – anti-CTLA-4, A – alisertib, C – combination. CTLA-4, cytotoxic T-lymphocyte associated protein 4, IO-Immunotherapy; PARP, poly(ADP-ribose) polymerase .

contributed to the improved antitumor efficacy seen with the combination of alisertib and anti-CTLA-4 compared with the anti-PD-1 combination.

In addition to causing direct tumor cell lysis, many standard-of-care chemotherapeutic reagents used for cancer treatment target immunosuppressive populations such as Tregs and MDSCs for depletion.[44–46] For example, paclitaxel, cyclophosphamide, and temozolomide have been reported to cause Treg depletion,[44 45] while doxorubicin and 5-fluorouracil have been reported to promote selective depletion of MDSCs.[47] Our data from both in vivo and ex vivo studies clearly established that Aurora A inhibition by alisertib resulted in the apoptotic depletion of MDSCs but not CD8 T cells in three different preclinical models of HPV-driven cancers (figure 4H, online supplemental figure S3). Our data suggest that Aurora A promoted an immunosuppressive TIME, which is supported by other studies. For example, in a mouse breast cancer model, inhibition of Aurora A led to apoptosis of MDSCs via reduced STAT3-mediated reactive oxygen species production.[48] The beneficial effects of Aurora A inhibition have also been supported in other cancer models.[49–52] Future studies could explore combinations with therapeutic HPV vaccines[53] or other immune checkpoint molecules that may activate effector T cells in HPV-driven[54] cancers.

The differential effect of alisertib on MDSCs compared with CD8 T cells observed in our study is intriguing and may be due to several factors, which warrant further investigation. First, MDSCs are often in a more proliferative state than resting CD8 T cells, making them potentially more susceptible to Aurora kinase inhibition. Additionally, MDSCs may rely more heavily on Aurora kinase for their survival and function compared with CD8 T cells. Another possibility is that alisertib's inhibition of STAT3-mediated reactive oxygen species production is more critical for MDSC survival than for CD8 T cells, as previously reported by Yin *et al*.[48] Finally, MDSCs are known to deplete amino acids essential for T-cell activation and proliferation,[55] which could also influence their distinct response to alisertib. These hypotheses underscore the need for further research to fully elucidate the mechanisms behind alisertib's selective effect on MDSCs in our model.

In the present study, we demonstrated that alisertib administration selectively and transiently depleted MDSCs from both the bloodstream and the tumor site at day 13 after tumor cell implantation. The decrease of MDSCs resulted in the systemic enrichment and activation of CD8 T cells, which played a substantial role in reducing the weight of HPV-positive cervical tumors by day 25 (figure 2B). Importantly, these reactions within the TIME due to Aurora A inhibition occurred before the tumor regressed, which supports the hypothesis that the reduction in MDSCs may have contributed to the recruitment and/or stimulation of tumor-reactive T cells.[18] Therefore, our findings illustrate that alisertib directly influenced the TIME by inhibiting MDSCs, which promote tumor growth, and restoring antitumor T cells.

MDSC-mediate immune suppression, tumor immune evasion, and contribute to tumor metastasis. Many studies have demonstrated that MDSCs are susceptible to cytotoxic chemotherapy.[56] In a separate study, inhibitors targeting tumor necrosis factor-related apoptosis-induced ligand receptors were employed to target MDSCs, resulting in some observed benefits.[57] However, the underlying mechanism is not clear. In this study, our findings revealed that ex vivo treatment of mEER cells from tumor-bearing mice with alisertib led to a pronounced induction of apoptosis in MDSCs (figure 3) accompanied by a significant increase in cytochrome C levels.

While our study demonstrates promising results in immunotherapy-resistant primary tumor models, we acknowledge a limitation in not addressing the effectiveness of this combination therapy in metastatic settings. Given that MDSCs play a crucial role in tumor immune evasion and metastasis, and our findings show the combination's ability to deplete MDSCs and enhance systemic immune responses, there is potential for this approach to be effective against distant metastatic disease.

In conclusion, this investigation establishes that Aurora A inhibition induces apoptosis, DNA damage, and ICD (specifically pyroptosis) in HPV-positive tumors. To our knowledge, this study is the first to demonstrate the immune-modulating effects of Aurora A inhibition in the context of HPV-positive tumors. Importantly, the research showed that alisertib enhanced the efficacy of ICIs targeting PD-1 or CTLA-4 in HPV-positive cancers, and the combination of alisertib and anti-CTLA-4 exhibited superior antitumor efficacy. The observed tumor regression was driven by both immune modulation and the direct reduction of tumor cell viability. The observed increased long-term survival, and enhanced CD8 T-cell responses underscore the potential efficacy of this combination therapy. Additionally, the study highlights alisertib's unique ability to selectively deplete MDSCs, contributing to efficient tumor regression and influencing the TIME. Our findings not only shed light on the novel immune-modulating effects of alisertib but also suggest that combining Aurora A inhibition with immune checkpoint blockade is a promising strategy for treating HPV-positive cancers.

Acknowledgements We thank Madison Semro, Associate Scientific Editor, and Stephanie Deming, Senior Scientific Editor, in the Research Medical Library at The University of Texas MD Anderson Cancer Center for editing this article.

Contributors SG: Conceptualization, validation, investigation, visualization, methodology, writing—original draft, writing—review and editing. MPO: Conceptualization, validation, investigation, visualization, methodology, writing—review and editing. TM: Investigation. PS: Investigation, methodology. LY: Investigation, writing—review and editing. JKS: Conceptualization, funding acquisition, project administration, supervision, writing—review and editing. FMJ: Conceptualization, funding acquisition, project administration, writing—review, editing and guarantor.

Funding This work was supported by the National Institutes of Health (R01CA248205 to FMJ and JKS). LY was supported by a training fellowship from UTHealth Houston's Center for Clinical and Translational Sciences TL1 Program

(grant no. TL1TR003169). We want to thank everyone in the Flow Cytometry & Cellular Imaging facility, which is supported in part by the NIH through MD Anderson's Cancer Center Support Grant P30CA016672.

Competing interests FMJ and JKS have received research funding from Takeda Pharmaceuticals. All other authors declare no potential conflicts of interest.

Patient consent for publication Not applicable.

Ethics approval All animal experiments were performed in accordance with the Guide for the Care and Use of Laboratory Animals from the National Institutes of Health and approved by the Institutional Animal Care and Use Committee of The University of Texas MD Anderson Cancer Center, protocol number 00000858-RN04.

Provenance and peer review Not commissioned; externally peer reviewed.

Data availability statement All data relevant to the study are included in the article or uploaded as supplementary information. The data generated in this study are available within the article and its Supplementary Data files. Any data used in this study that are not included in the paper or supplementary files can be made available upon request from the corresponding author.

ORCID iDs
Jagannadha K Sastry http://orcid.org/0000-0002-6987-4422
Faye M Johnson http://orcid.org/0000-0002-2862-4160

REFERENCES

1 Mahal BA, Catalano PJ, Haddad RI, *et al*. Incidence and Demographic Burden of HPV-Associated Oropharyngeal Head and Neck Cancers in the United States. *Cancer Epidemiol Biomarkers Prev* 2019;28:1660–7.
2 Aggarwal P, Zaveri JS, Goepfert RP, *et al*. Swallowing-related outcomes associated with late lower cranial neuropathy in long-term oropharyngeal cancer survivors: cross-sectional survey analysis. *Head Neck* 2019;41:3880–94.
3 Ghosh S, Shah PA, Johnson FM. Novel Systemic Treatment Modalities Including Immunotherapy and Molecular Targeted Therapy for Recurrent and Metastatic Head and Neck Squamous Cell Carcinoma. *Int J Mol Sci* 2022;23:7889.
4 Burtness B, Harrington KJ, Greil R, *et al*. Pembrolizumab alone or with chemotherapy versus cetuximab with chemotherapy for recurrent or metastatic squamous cell carcinoma of the head and neck (KEYNOTE-048): a randomised, open-label, phase 3 study. *Lancet* 2019;394:1915–28.
5 Monk BJ, Enomoto T, Kast WM, *et al*. Integration of immunotherapy into treatment of cervical cancer: Recent data and ongoing trials. *Cancer Treat Rev* 2022;106:102385.
6 Ott PA, Piha-Paul SA, Munster P, *et al*. Safety and antitumor activity of the anti-PD-1 antibody pembrolizumab in patients with recurrent carcinoma of the anal canal. *Ann Oncol* 2017;28:1036–41.
7 Morris VK, Salem ME, Nimeiri H, *et al*. Nivolumab for previously treated unresectable metastatic anal cancer (NCI9673): a multicentre, single-arm, phase 2 study. *Lancet Oncol* 2017;18:446–53.
8 Ferris RL, Blumenschein G Jr, Fayette J, *et al*. Nivolumab for Recurrent Squamous-Cell Carcinoma of the Head and Neck. *N Engl J Med* 2016;375:1856–67.
9 Ferris RL, Blumenschein G Jr, Fayette J, *et al*. Nivolumab vs investigator's choice in recurrent or metastatic squamous cell carcinoma of the head and neck: 2-year long-term survival update of CheckMate 141 with analyses by tumor PD-L1 expression. *Oral Oncol* 2018;81:45–51.
10 Garassino MC, Gadgeel S, Speranza G, *et al*. Pembrolizumab Plus Pemetrexed and Platinum in Nonsquamous Non-Small-Cell Lung Cancer: 5-Year Outcomes From the Phase 3 KEYNOTE-189 Study. *J Clin Oncol* 2023;41:1992–8.
11 Novello S, Kowalski DM, Luft A, *et al*. Pembrolizumab Plus Chemotherapy in Squamous Non-Small-Cell Lung Cancer: 5-Year Update of the Phase III KEYNOTE-407 Study. *J Clin Oncol* 2023;41:1999–2006.
12 Topalian SL, Sznol M, McDermott DF, *et al*. Survival, durable tumor remission, and long-term safety in patients with advanced melanoma receiving nivolumab. *J Clin Oncol* 2014;32:1020–30.
13 Mehra R, Seiwert TY, Gupta S, *et al*. Efficacy and safety of pembrolizumab in recurrent/metastatic head and neck squamous cell carcinoma: pooled analyses after long-term follow-up in KEYNOTE-012. *Br J Cancer* 2018;119:153–9.
14 Galluzzi L, Buqué A, Kepp O, *et al*. Immunogenic cell death in cancer and infectious disease. *Nat Rev Immunol* 2017;17:97–111.
15 Zhang Z, Zhang Y, Xia S, *et al*. Gasdermin E suppresses tumour growth by activating anti-tumour immunity. *Nature New Biol* 2020;579:415–20.
16 Ghosh S, Mazumdar T, Xu W, *et al*. Combined TRIP13 and Aurora Kinase Inhibition Induces Apoptosis in Human Papillomavirus-Driven Cancers. *Clin Cancer Res* 2022;28:4479–93.
17 Lee JW, Parameswaran J, Sandoval-Schaefer T, *et al*. Combined Aurora Kinase A (AURKA) and WEE1 Inhibition Demonstrates Synergistic Antitumor Effect in Squamous Cell Carcinoma of the Head and Neck. *Clin Cancer Res* 2019;25:3430–42.
18 Vilgelm AE, Johnson CA, Prasad N, *et al*. Connecting the Dots: Therapy-Induced Senescence and a Tumor-Suppressive Immune Microenvironment. *J Natl Cancer Inst* 2016;108:djv406.
19 Haddad TC, Suman VJ, D'Assoro AB, *et al*. Evaluation of Alisertib Alone or Combined With Fulvestrant in Patients With Endocrine-Resistant Advanced Breast Cancer: The Phase 2 TBCRC041 Randomized Clinical Trial. *JAMA Oncol* 2023;9:815–24.
20 Melichar B, Adenis A, Lockhart AC, *et al*. Safety and activity of alisertib, an investigational aurora kinase A inhibitor, in patients with breast cancer, small-cell lung cancer, non-small-cell lung cancer, head and neck squamous-cell carcinoma, and gastro-oesophageal adenocarcinoma: a five-arm phase 2 study. *Lancet Oncol* 2015;16:395–405.
21 Dorta-Estremera S, Hegde VL, Slay RB, *et al*. Targeting interferon signaling and CTLA-4 enhance the therapeutic efficacy of anti-PD-1 immunotherapy in preclinical model of HPV$^+$ oral cancer. *J Immunother Cancer* 2019;7:252.
22 Dorta-Estremera S, Chin RL, Sierra G, *et al*. Mucosal HPV E6/E7 Peptide Vaccination in Combination with Immune Checkpoint Modulation Induces Regression of HPV$^+$ Oral Cancers. *Cancer Res* 2018;78:5327–39.
23 Sierra G, Dorta-Estremera S, Hegde VL, *et al*. Intranasal Therapeutic Peptide Vaccine Promotes Efficient Induction and Trafficking of Cytotoxic T Cell Response for the Clearance of HPV Vaginal Tumors. *Vaccines (Basel)* 2020;8:259.
24 Palani S, Patel M, Huck J, *et al*. Preclinical pharmacokinetic/pharmacodynamic/efficacy relationships for alisertib, an investigational small-molecule inhibitor of Aurora A kinase. *Cancer Chemother Pharmacol* 2013;72:1255–64.
25 Zhao M, Sano D, Pickering CR, *et al*. Assembly and initial characterization of a panel of 85 genomically validated cell lines from diverse head and neck tumor sites. *Clin Cancer Res* 2011;17:7248–64.
26 Williams R, Lee DW, Elzey BD, *et al*. Preclinical models of HPV+ and HPV– HNSCC in mice: An immune clearance of HPV+ HNSCC. *Head & Neck* 2009;31:911–8.
27 Smith KA, Meisenburg BL, Tam VL, *et al*. Lymph Node–Targeted Immunotherapy Mediates Potent Immunity Resulting in Regression of Isolated or Metastatic Human Papillomavirus–Transformed Tumors. *Clin Cancer Res* 2009;15:6167–76.
28 Ji H, Chang EY, Lin KY, *et al*. Antigen-specific immunotherapy for murine lung metastatic tumors expressing human papillomavirus type 16 E7 oncoprotein. *Int J Cancer* 1998;78:41–5.
29 Ferrarotto R, Goonatilake R, Young Yoo S, *et al*. Epithelial–Mesenchymal Transition Predicts Polo-Like Kinase 1 Inhibitor–Mediated Apoptosis in Non–Small Cell Lung Cancer. *Clin Cancer Res* 2016;22:1674–86.
30 Kalu NN, Mazumdar T, Peng S, *et al*. Genomic characterization of human papillomavirus-positive and -negative human squamous cell cancer cell lines. *Oncotarget* 2017;8:86369–83.
31 Schneider CA, Rasband WS, Eliceiri KW. NIH Image to ImageJ: 25 years of image analysis. *Nat Methods* 2012;9:671–5.
32 Teilmann AC, Nygaard Madsen A, Holst B, *et al*. Physiological and pathological impact of blood sampling by retro-bulbar sinus

puncture and facial vein phlebotomy in laboratory mice. *PLoS One* 2014;9:e113225.
33 Bartkowiak T, Singh S, Yang G, *et al*. Unique potential of 4-1BB agonist antibody to promote durable regression of HPV+ tumors when combined with an E6/E7 peptide vaccine. *Proc Natl Acad Sci U S A* 2015;112:E5290–9.
34 Jiang M, Qi L, Li L, *et al*. The caspase-3/GSDME signal pathway as a switch between apoptosis and pyroptosis in cancer. *Cell Death Discov* 2020;6:112.
35 Obeid M, Tesniere A, Ghiringhelli F, *et al*. Calreticulin exposure dictates the immunogenicity of cancer cell death. *Nat Med* 2007;13:54–61.
36 Fucikova J, Becht E, Iribarren K, *et al*. Calreticulin Expression in Human Non-Small Cell Lung Cancers Correlates with Increased Accumulation of Antitumor Immune Cells and Favorable Prognosis. *Cancer Res* 2016;76:1746–56.
37 Cervantes A, Elez E, Roda D, *et al*. Phase I pharmacokinetic/pharmacodynamic study of MLN8237, an investigational, oral, selective aurora a kinase inhibitor, in patients with advanced solid tumors. *Clin Cancer Res* 2012;18:4764–74.
38 Ding Y-H, Zhou Z-W, Ha C-F, *et al*. Alisertib, an Aurora kinase A inhibitor, induces apoptosis and autophagy but inhibits epithelial to mesenchymal transition in human epithelial ovarian cancer cells. *Drug Des Devel Ther* 2015;9:425–64.
39 Youn JI, Gabrilovich DI. The biology of myeloid-derived suppressor cells: the blessing and the curse of morphological and functional heterogeneity. *Eur J Immunol* 2010;40:2969–75.
40 Clavijo PE, Moore EC, Chen J, *et al*. Resistance to CTLA-4 checkpoint inhibition reversed through selective elimination of granulocytic myeloid cells. *Oncotarget* 2017;8:55804–20.
41 Selby MJ, Engelhardt JJ, Quigley M, *et al*. Anti-CTLA-4 antibodies of IgG2a isotype enhance antitumor activity through reduction of intratumoral regulatory T cells. *Cancer Immunol Res* 2013;1:32–42.
42 Ruffin AT, Li H, Vujanovic L, *et al*. Improving head and neck cancer therapies by immunomodulation of the tumour microenvironment. *Nat Rev Cancer* 2023;23:173–88.
43 Peggs KS, Quezada SA, Chambers CA, *et al*. Blockade of CTLA-4 on both effector and regulatory T cell compartments contributes to the antitumor activity of anti-CTLA-4 antibodies. *J Exp Med* 2009;206:1717–25.
44 Vincent J, Mignot G, Chalmin F, *et al*. 5-Fluorouracil selectively kills tumor-associated myeloid-derived suppressor cells resulting in enhanced T cell-dependent antitumor immunity. *Cancer Res* 2010;70:3052–61.
45 Ridolfi L, Petrini M, Granato AM, *et al*. Low-dose temozolomide before dendritic-cell vaccination reduces (specifically) CD4+CD25++Foxp3+ regulatory T-cells in advanced melanoma patients. *J Transl Med* 2013;11:135.
46 Opzoomer JW, Sosnowska D, Anstee JE, *et al*. Cytotoxic Chemotherapy as an Immune Stimulus: A Molecular Perspective on Turning Up the Immunological Heat on Cancer. *Front Immunol* 2019;10:1654.
47 Alizadeh D, Trad M, Hanke NT, *et al*. Doxorubicin eliminates myeloid-derived suppressor cells and enhances the efficacy of adoptive T-cell transfer in breast cancer. *Cancer Res* 2014;74:104–18.
48 Yin T, Zhao Z-B, Guo J, *et al*. Aurora A Inhibition Eliminates Myeloid Cell-Mediated Immunosuppression and Enhances the Efficacy of Anti-PD-L1 Therapy in Breast Cancer. *Cancer Res* 2019;79:3431–44.
49 Zheng D, Li J, Yan H, *et al*. Emerging roles of Aurora-A kinase in cancer therapy resistance. *Acta Pharm Sin B* 2023;13:2826–43.
50 Sun S, Zhou W, Li X, *et al*. Nuclear Aurora kinase A triggers programmed death-ligand 1-mediated immune suppression by activating MYC transcription in triple-negative breast cancer. *Cancer Commun* 2021;41:851–66.
51 Tatsuka M, Sato S, Kanda A, *et al*. Oncogenic role of nuclear accumulated Aurora-A. *Mol Carcinog* 2009;48:810–20.
52 Zheng F, Yue C, Li G, *et al*. Nuclear AURKA acquires kinase-independent transactivating function to enhance breast cancer stem cell phenotype. *Nat Commun* 2016;7:10180.
53 Massarelli E, William W, Johnson F, *et al*. Combining Immune Checkpoint Blockade and Tumor-Specific Vaccine for Patients With Incurable Human Papillomavirus 16-Related Cancer: A Phase 2 Clinical Trial. *JAMA Oncol* 2019;5:67–73.
54 Baudouin R, Tartour E, Badoual C, *et al*. Hypothesis of a CD137/Eomes activating axis for effector T cells in HPV oropharyngeal cancers. *Mol Med* 2024;30:26.
55 Yang Y, Li C, Liu T, *et al*. Myeloid-Derived Suppressor Cells in Tumors: From Mechanisms to Antigen Specificity and Microenvironmental Regulation. *Front Immunol* 2020;11:1371.
56 Okwuone DDD, Morgan D, Gan GN. Exploring the function of myeloid cells in promoting metastasis in head and neck cancer. *Explor Target Antitumor Ther* 2024;5:108–19.
57 Dominguez GA, Condamine T, Mony S, *et al*. Selective Targeting of Myeloid-Derived Suppressor Cells in Cancer Patients Using DS-8273a, an Agonistic TRAIL-R2 Antibody. *Clin Cancer Res* 2017;23:2942–50.